

## Two-Dimensional Simulation of Electrostatic Field for Electrical Resistance Tomography

K L Ostrowski and R A Williams

Particle and Colloid Engineering Group, Camborne School of Mines, University of Exeter  
Redruth, Cornwall TR15 3SE UK  
Tel:(+44)01209 714866, Fax: (+44) 01209 716977, E-mail: williams@csm.ex.ac.uk

**Abstract** – *The two-dimensional analysis of the electrostatic field inside an electrical resistance tomography sensor is presented. The theoretical model is based on application of the logarithmic potential to the surface of each electrode transformed by conformal mapping from sensor circumference to a straight line. This approach automatically returns singularities at the edge points of each electrode. Examples of voltage and current function distribution are given for different electrode angles and different positions of the source and sink electrodes.*

**Keywords** : electrical tomography, field simulation, analytical functions, logarithmic potential

### 1. INTRODUCTION

Calculation of electrostatic field in the interior of the electrical tomography sensor is of particular importance when Linear Back Projection (LBP) is used to obtain reconstructed image, since the *sensitivity maps* are just determined solely by the results of field simulation. In addition it provides e.g. basis to sensor optimisation by predicting calibration data. Standard simplifications applied to Maxwell's equations lead to the mathematical problem which consists of second order partial differential equation of elliptic type – Poisson, Laplace (considered in this paper) or Helmholtz (in the case of homogenous medium) with boundary conditions imposed on the wall of the domain being considered.

In the case of electrical resistance tomography (ERT) the main discrepancies between particular physical and mathematical models result from the differences in the electrodes simulations. Typical models which can be found in the literature [1, 2] such as 'point electrodes model', 'gap model', 'shunt model' and 'complete model' just differ by the method used for simulation of the electrodes and also the physical phenomena that occur on their surfaces.

Application of the logarithmic potential to the shunt model leads to the set of  $N$  (where  $N$  is the number of electrodes) integral equations of the Fredholm type with the  $N$  unknown distribution of logarithmic potential. The method of solution strongly depends on this expected distribution. The logarithmic potential may be expanded e.g. into a Fourier series.

Since the shunt model neglects surface resistance we simplified the problem assuming that the potential has to be equal at the edge points of each electrode only. This approach provides a relatively simple solution which provides prompt, but not completely accurate information, on the electrostatic field distribution.

### 2. MODELS AND BOUNDARY CONDITIONS

The method of the electrode simulation is equivalent to the selection of proper boundary conditions for the Laplace equation.

It is commonly agreed that boundary conditions imposed on the part of sensor circumference that is not occupied by electrodes are of the Neumann type:

$$\frac{\partial \Phi}{\partial n} = 0 \quad (1)$$

Where  $\Phi$  is potential (voltage) and  $n$  is direction normal to sensor circumference. Condition (1) is common for all models.

The difference between particular models lies in the boundary conditions on the electrode surfaces. In the point model active electrodes are simulated by the strong singularities (source and sink) while the detecting electrodes do not exist.

In the gap model uniform distribution of current density is postulated i.e. current density for each electrode is constant and equal to:

$$j_n = \frac{I_n}{e_n} \tag{2}$$

Where  $j$  is the current density,  $I$  total current,  $e$  electrode width and  $n$  index of electrode respectively. Again since the total current is equal to zero for each detecting electrode these electrodes do not exist in this model.

In the shunt model the boundary conditions for each electrode are as follow:

$$I_n \text{ is known for each electrode} \tag{3a}$$

$$\Phi = \text{const (but unknown)} \tag{3b}$$

The second condition (3b) results from the assumption that electrical conductivity  $\sigma$  is, in practice, infinite for an electrode (metal) when compared with the range of the conductivity of the media being tested.

Finally the complete model includes a surface impedance term  $\rho$ . Thus boundary conditions (3) are replaced by:

$$I_n \text{ is known for each electrode} \tag{4}$$

$$\Phi_n + j_n \rho = \text{const (but unknown)}$$

Impedance is usually assumed to be constant. Current density  $j_n$  varies along the electrode surface.

The completed model meets the experimental data best [ 3 ]. This however requires the proper selection an unknown *a priori* value of impedance.

It is essential that the two last models yield singularities at the edge points of electrodes because of a rapid change of boundary conditions. Thus the orthogonal series (usually Fourier series) describing, for example, voltage distribution on the sensor boundary have a relatively poor convergence.

The main purpose of this contribution is to propose a method which imposes this singularities on the electrode edges and then the exact solution may be obtained by *superposition* with continuous function obeying the Dirichlet condition. The first step of this method is presented in the next section.

### 3. SOLUTION

#### 3.1 The logarithmic potential

One of the possible methods for looking for an analytical function  $f(z)$  on a complex plane:

$$z = x + iy$$

(where  $i$  is an imaginary unit), is to introduce a continuous distribution of singularities, namely vortices and sources along a given line or lines. Thus an analytical function  $f(z)$  is given in the form:

$$f(z) = \Phi + i\Psi = \int_1 \gamma(l_o) \ln(z - z_o) dl_o \tag{5}$$

where  $\Psi$  is a current (stream) function,  $l$  is the line singularities are imposed on and  $\gamma$  represents the density of singularities. In the general case  $\gamma$  may be complex i.e. the singularity consists of both sources and vortices.

The derivative of  $f(z)$  is thus given by the relation:

$$\frac{df(z)}{dz} = \int_1 \frac{\gamma(l_o)}{z - z_o} dl_o \tag{6}$$

The general theory of logarithmic potential may be found for example in [4, 5]. One of classical application is given by Glauert [6], who applied this method to simulate flow past a thin aerofoil. He expanded the density function into a Fourier series and then calculated the total circulation around its profile.

#### 3.2 Mapping of the sensor cross-section

In the first step the circular interior of the ERT sensor is mapped into a half-plane:

$$w = u + iv$$

according to relation:

$$z = \frac{1 - w}{1 + w} \tag{7a}$$

or, alternatively:

$$w = i \frac{1 - z}{1 + z} \tag{7b}$$

Figure 1 show this mapping, according to which any point placed on the circumference of the unit circle on  $z$  plane is transformed on the real axis  $u$  on the  $w$  plane:

$$\eta = \frac{\sin \alpha}{1 + \cos \alpha} \quad (8)$$

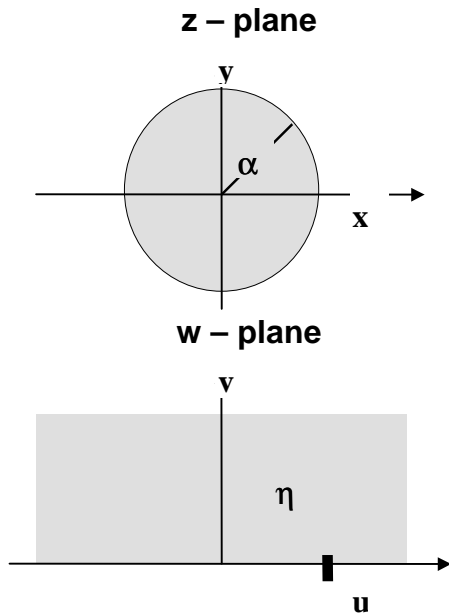


Figure 1: Mapping a unit circle onto a half plane

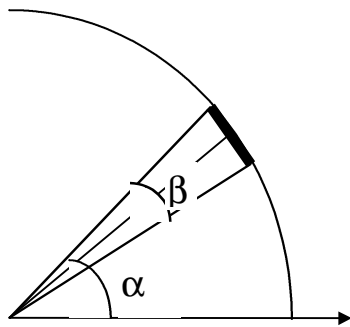


Figure 2: Electrode position on z plane

On the z plane the position of each electrode can be determined by two angles determining (for example centre of the electrode ( $\alpha$ ) and its width ( $\beta$ )). Then on w plane each electrode is a straight segment occupying part of real axis which characteristic points may be calculating by means of equation (8).

### 3.3 Approximate solution of the shunt model

Due to linearity of Laplace equation is useful to consider the normalized solution i.e. for unit injected current and unit electrical conductivity (or resistivity). Multiplying the normalized voltage (potential) by actual value of current and dividing by value of conductivity it is easy to obtain a real value of voltage.

In the first step the basic field is created by imposing on the source and sink electrodes the analytical functions given by the relation:

$$w = \pm e_w \cosh(f_0(w) / \pi) \quad (9)$$

where  $e_w$  is the width of the source or sink electrode of w plane and  $f_0(w)$  describes the complex potential resulting from injection of single current to a half plane shown in figure 1. The detailed description of function given by equation (9) may be found in literature [4, 5]. Here we only point out that streamlines are confocal hyperbolas, whose foci are  $(e_w, 0)$  and  $(-e_w, 0)$ , while lines of constant potential are ellipses having the same foci.

Function  $f_0(w)$  obeys conditions (1) and (3a). Potential however is not constant on the electrode surfaces. Thus in the next step an additional analytical function should be imposed to create a *superposition* which also obeys condition (3b). This function should not spoil the properties of the basic field since it should also obey condition (1) and not generate a total current on the surface of any electrode. Following the concept of the logarithmic potential described briefly in section 3.1 a continuous distribution of sources and sinks can be imposed on the surface of each electrode.

Such distributions automatically obey condition (1) (no component of current density normal to the real axis is generated) while condition (3a) is now expressed as:

$$\int_{ew} \gamma(u) du = 0 \quad \text{for each electrode} \quad (10)$$

Condition (3b) can now be written in the form:

$$\left. \frac{df_0(w)}{dw} \right|_{n=1} = - \sum_{N_{ew}} \int \frac{\gamma_n(u_o)}{w - w_o} du_o$$

.to

$$\left. \frac{df_0(w)}{dw} \right|_{n=N} = - \sum_{N_{ew}} \int \frac{\gamma_n(u_o)}{w - w_o} du_o \quad (11)$$

That is a set of N Fredholm equations. The sum of interactions coming from distribution for each electrode should cancel the tangential component of potential derivative on the surface of each electrode. An additional difficulty results from the fact that a kernel in one term in the integrals sum on right hand side of (11) has a strong singularity.

Below we will use some results derived by Glauert with a small modification. For each segment on u axis representing particular electrode is possible to introduce auxiliary variable  $\phi$  according to the definition:

$$u = \frac{e_w}{2} (1 - \cos \varphi) = e_w \sin^2 \frac{\varphi}{2} \quad (12)$$

Thus for each electrode on  $w$  plane  $\varphi$  varies from 0 to  $\pi$ .

Now the function  $\gamma(u) = \gamma(\varphi)$  may be presented in the form:

$$\gamma(\varphi) = A_0 \cot \varphi + \sum_{m=2}^{\infty} A_m \sin(m\varphi) + \sum_{m=2}^{\infty} B_m \cos(m\varphi) \quad (13)$$

In the Fourier series on the right hand side of (13) all terms which return nonzero total positive or negative source distribution have to be removed.

The only term which returns singularities at the edge points of electrode is the first one on the right hand side of (13). In the present analysis the influence of this term is considered. It can be proved that the term  $\cot \varphi$  returns the linear potential distribution on each segment on the  $u$  axis. The analytical function describing the potential and stream function distribution associated with this term has the form:

$$f(w) = A \left\{ \sqrt{(w - e_{wcn})^2 - e_{wn}^2} - w \right\} \quad (14)$$

where  $A$  is arbitrary constant,  $e_{wcn}$  is the central point of the  $n$ th electrode on  $w$  plane and  $e_{wn}$  is the length of the segment on  $u$  axis representing the  $n$ th electrode, respectively.

Finally, the total complex potential obtained from our model may be expressed as:

$$\Phi + i\Psi = f_0(w) + \sum_{n=1}^N A_n \left\{ \sqrt{(w - e_{wcn})^2 - e_{wn}^2} - w \right\} \quad (15)$$

It is convenient to select source and sink electrodes to be placed symmetrically versus the  $x$  axis on  $z$  plane. Then their images on the  $w$  plane are placed symmetrically along the  $v$  axis and number of unknown coefficients  $A_n$  is reduced to  $N/2$ . The method of their calculation strongly depend on number of electrodes  $N$ . For a standard value  $N=16$  a simple iteration method has been applied.

In the first step the coefficient  $A_n$  are calculated starting from the voltage distribution resulting from the basic field. Then a new field is calculated as well as voltage differences at the edge points for each electrode resulting from. The new set of functions (14) provide the next normalized voltage distribution on the circumference of the sensor. Typically four

iterations may be required for  $N = 16$  and an electrode angle  $\beta < 15^\circ$ .

### 4. RESULTS

Solution of equation (15) provides the value of normalized voltage (potential) and normalized stream (current) function at any point of the sensor cross-section. These values, notably on the sensor boundary, may be predicted to estimate shunt effect and thus select an appropriate value for the electrode angle  $\beta$ .

Figures 3 – 8 show typical distributions of the potential and stream function provided by model. The source and sink electrodes are placed symmetrically versus the  $x$  axis so only half of sensor circumference has to be shown.

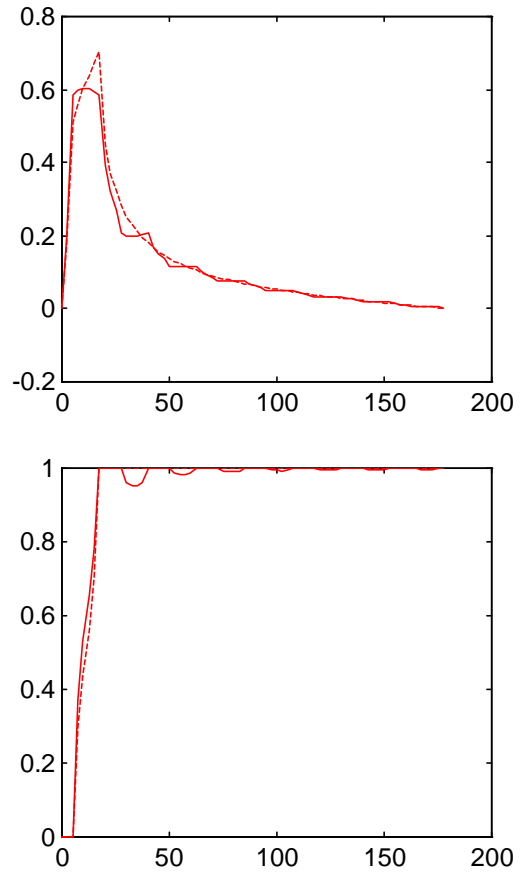


Figure 3: Distribution of normalized voltage (top) and normalized stream (current) function (bottom) vs. angle (deg). Dotted line shows the basic solution and solid line the final solution of equation (15).  $N=16$ ,  $\beta = 12.5^\circ$  (56% of sensor circumference is occupied by electrodes). Source and sink electrodes are adjacent.

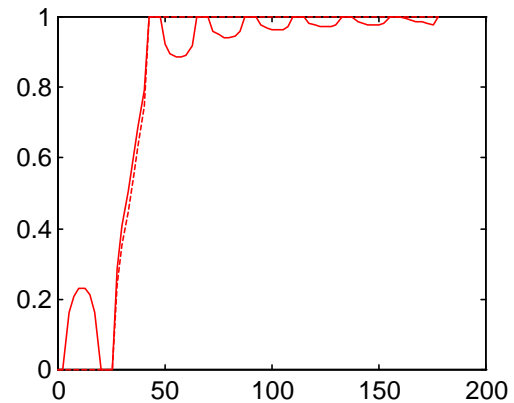
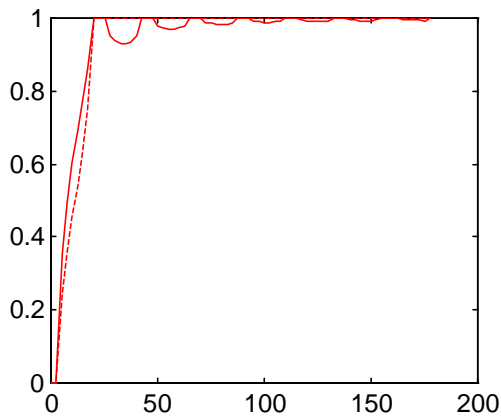
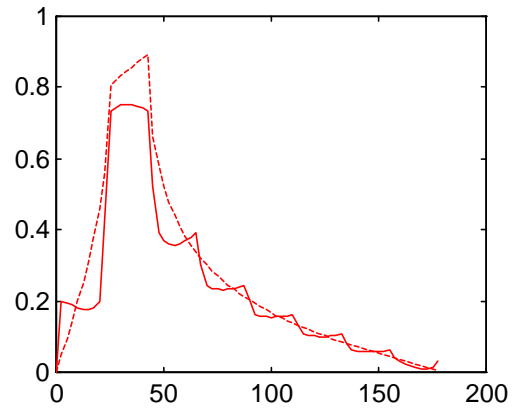
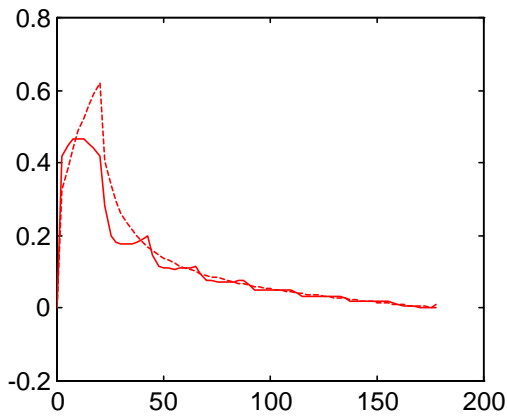


Figure 4: Distribution of normalized voltage (top) and normalized stream (current) function (bottom) vs. angle (deg). Dotted line shows the basic solution and solid line the final solution of equation (15).  $N=16$ ,  $\beta = 17.5^\circ$  (78% of sensor circumference is occupied by electrodes). Source and sink electrodes are adjacent.

Figure 6: Distribution of normalized voltage (top) and normalized stream (current) function (bottom) vs. angle (deg). Dotted line shows the basic solution and solid line the final solution of equation (15).  $N=16$ ,  $\beta = 17.5^\circ$  (78% of sensor circumference is occupied by electrodes). Source and sink electrodes are separated by two electrodes

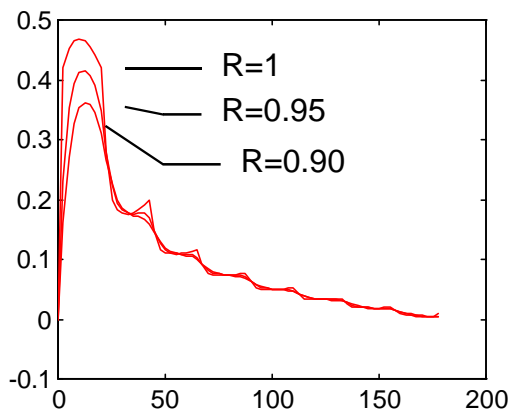


Figure 5: Distribution of normalized voltage vs. angle (deg) for three values of normalized radius,  $R = 1, 0.95, 0.90$ .  $N=16$ ,  $\beta = 17.5^\circ$  (78% of sensor circumference is occupied by electrodes). Source and sink electrodes are adjacent.

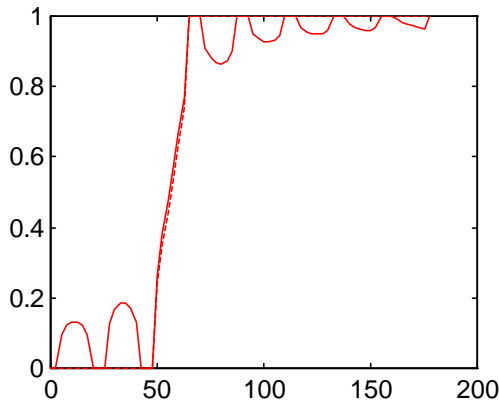
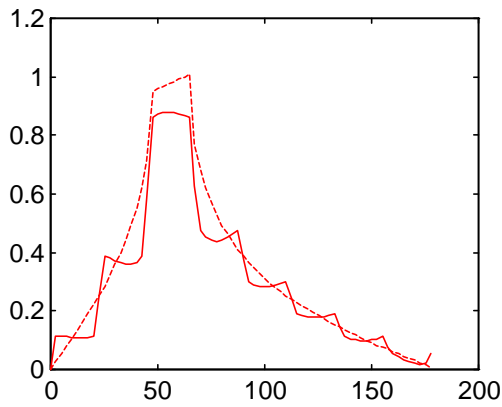


Figure 7: Distribution of normalized voltage (top) and normalized stream (current) function (bottom) vs. angle (deg). Dotted line shows the basic solution and solid line the final solution of equation (15).  $N=16$ ,  $\beta = 17.5^\circ$  (78% of sensor circumference is occupied by electrodes). Source and sink electrodes are separated by four electrodes.

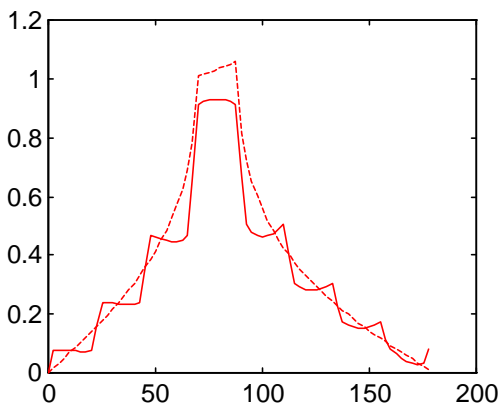


Figure 8 a: Distribution of normalized voltage vs. angle (deg). Dotted line shows the basic solution and solid line the final solution of equation (15).  $N=16$ ,  $\beta = 17.5^\circ$ . Source and sink electrodes are separated by six electrodes

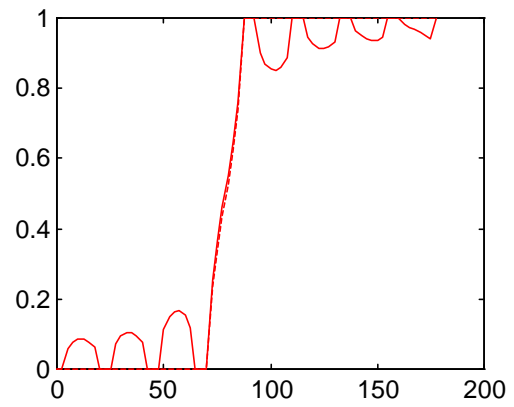


Figure 8 b: Distribution of normalized stream function for sensor parameters the same as in figure 8a.

## 5. CONCLUSIONS AND FUTURE WORK

This paper shows how the logarithmic potential may be applied to simulate electrostatic field inside an ERT sensor. This model is restricted to 2-D field simulation which produces some errors in field description. Since however this model is relatively simple and fast (four iterations provide the accurate solution for the first component of the Legendre's function of the first order) the presented analysis was restricted to this approximation.

Figure 5 shows voltage distributions for three values of normalized radius ( $R = 1$  corresponds with sensor boundary). It is clearly shown that the inaccuracies resulting from the assumed simplification disappear rapidly with distance from the sensor boundary. This fact justifies the approach we have taken to reach the solution.

Distributions of the stream function show shunt effect for various positions of the source and the sink electrodes. The maximum effect occurs when these electrodes are separated by two electrode distances (figure 6). Approximately 25 percent of total injected current flows through electrodes.

In future work the solution will be directly applied to the sensitivity calculations at any point of sensor cross-section for various electrode angles, various number of electrodes and particular combinations of active and detecting electrodes.

## ACKNOWLEDGMENTS

The authors acknowledge the support of the UK Engineering and Physical Sciences Council through grant GR/K 89146.

## REFERENCES

- [1] M S Beck, M Morris, R C Waterfall, R A Williams and E Campograde, "Tomographic Techniques for Process Design and Operation", (Southampton: Computational Mechanics Publications), 1992.
- [2] M Wang, F J Dickin and M S Beck, "Improved Electrical Impedance Tomography Data Collection System and Measurement Protocol", "Tomographic Techniques for Process Design and Operation", ed M S Beck, E Campograde, R A Williams and R C Waterfall, (Southampton: Computational Mechanics Publications), 1992.
- [3] E Somersalo, M Cheney and D Isaacson, "Existence and Uniqueness for Electrode Models for Electric Current Computed Tomography", *J. Appl. Math.*, 1992, Vol. 52, No. 4, pp. 1023–1040.
- [4] L M Milne–Thomson, "Theoretical Hydrodynamics", 5th ed, The Macmillan Press, London, 1968.
- [5] H Lamb, "Hydrodynamics", Cambridge University Press, London – Dover, 1945.
- [6] H Glauert, "The Elements of Aerofoil and Airscrew Theory", Cambridge University Press, London, 1948.